Experimental Eye Research 91 (2010) 300–307

Contents lists available at ScienceDirect

Experimental Eye Research

journal homepage: www.elsevier.com/locate/yexer

Mouse lens stiffness measurements

Hussein Baradia, Negin Nikahd, Adrian Glasser*

College of Optometry, University of Houston, Houston, TX 77204, USA

ARTICLE INFO

Article history:
Received 4 December 2009
Accepted in revised form 7 June 2010
Available online 11 June 2010

Keywords:
lens stiffness
presbyopia
aging
force
accommodation

ABSTRACT

Presbyopia is a gradual loss of accommodation with age. Various studies have shown that an age-related increase in lens stiffness may be one factor involved. Lens stiffness has previously been measured using lens spinning experiments, resistance to conical probe penetration and dynamic mechanical analysis. In the current study, two different techniques have been used to evaluate the stiffness of isolated mouse lenses. In the first method, compressive forces were applied to mouse lenses using microscope cover-slips to exert incremental forces on the lens. Lens images were captured for analysis of change in diameter. In the second method, a fully automated squeezer system with an actuator, electronic scale and a CCD camera was used to apply incremental compressive forces to the lenses. The actuator exerted forces comparable to those exerted by cover-slips. Force and actuator displacement data together with images of the lenses as they were compressed were captured. Images were analyzed for change in lens diameter on application of force and also with actuator displacement. Lenses from 19 young male mice (4-weeks old) and 28 male retired breeders (7–9 months old) were tested. Lenses were used immediately after sacrificing the mice and extracting the lenses. The lenses from the older male mice were stiffer compared to the lenses from the younger male mice. This was determined by comparing the average change in lens diameter at various force values used. The two methods provide a good indication of the stiffness properties of mouse lenses.

1. Introduction

Several studies have suggested that presbyopia, the age-related loss of accommodative ability, is linked to an age-related increase in stiffness of the lens (Glasser and Campbell, 1999; Heys et al., 2004; Weeber et al., 2005, 2007). Various techniques have been used to show the age-related increase in stiffness of human lenses including spinning of lenses (Fisher, 1971; Krueger et al., 2001), resistance to conical probe penetration (Pau and Kranz, 1991), actuator squeezing (Glasser and Campbell, 1998), dynamic mechanical analysis (DMA) (Heys et al., 2004; Weeber et al., 2007) and bubble-based acoustic radiation force (Hollman et al., 2007). Here, two different squeezing methods have been used to measure stiffness of lenses from male mice of two different age groups.

Stiffness is the resistance that an elastic body offers to deformation by an applied force. Both compressive and extensive forces have been used to test lens stiffness. The natural change in shape of the young primate lens during accommodation is due to forces exerted by the capsule. In the unaccommodated eye, the lens is held in a relatively flattened state through zonular tension at the lens equator. When the ciliary muscle contracts, the zonular tension is released and the elastic capsule surrounding the lens causes the lens equatorial diameter to decrease and lens axial thickness to increase. Relaxation of the ciliary muscle increases zonular tension at the lens equator to pull the lens into a relatively flattened and unaccommodated state. The age-related increase in stiffness of the human lens has been measured using compressive, extensive or indentation forces (Fisher, 1971; Pau and Kranz, 1991; Glasser and Campbell, 1999; Heys et al., 2004; Weeber et al., 2007).

Mice are not known to accommodate or develop presbyopia. The mouse lens is nearly spherical and relatively stiffer than lenses from animal species known to accommodate. The mouse eye has a diminutive ciliary muscle that is not likely capable of changing the lens curvature or translating the lens in the eye to produce accommodation. Further, mice are nocturnal and rely heavily on olfactory cues and therefore may have little need for or benefit from accommodation. Mouse lenses have been used in this study to ascertain if the stiffness of mouse lenses increases with age. Mice are relatively inexpensive, widely available, they age rapidly, offer genetic opportunities and the lenses are small thereby allowing the possibility that mouse lenses could be maintained and treated in organ culture conditions and treated with pharmacological agents. If mouse lenses do undergo an age-related increase in stiffness, they could offer an opportunity for evaluating drugs or procedures that could be used to

* Corresponding author. Tel.: +1 713 743 1876; fax: +1 713 743 2053.
E-mail address: aglasser@uh.edu (A. Glasser).

0014-4835/$ – see front matter © 2010 Elsevier Ltd. All rights reserved.
doi:10.1016/j.exer.2010.06.003

soften the lens in efforts to restore accommodation or reverse presbyopia. A recent preliminary study has reported an age dependent increase in stiffness of mouse lenses (Sistla et al., 2009).

Few studies have measured mouse lens stiffness so the methodology to do this is not well described or validated. The testing performed here was designed to provide a repeatable method of testing mouse lens stiffness. The methods described could also be generalized to lenses from other species for understanding age related changes in the lens and presbyopia reversal procedures.

2. Methods

2.1. Animals

This study was performed in accordance with the ARVO Statement for the Use of Animals in Research and under an institutionally approved animal protocol. Mice were either group or singly housed in a 12/12 light/dark cycle with ad libertum food and water. Mice ordered were C57BL/6J (Jackson Laboratory, Bar Harbor, ME) either 4 weeks old male ($n = 19$) or 7–9 months old male retired breeders ($n = 28$). Mice were euthanized by carbon dioxide asphyxiation followed by cervical dislocation.

2.2. Lens dissection

Both eyes from each mouse were enucleated and placed in a chamber containing room temperature Hank's balanced salt solution (HBSS) with antibiotics. A liter of HBSS was supplemented with 1x of antibiotic-antimycotic (1000 units of penicillin (base), 1000 μg of streptomycin (base) and 2.5 μg of amphotericin B/ml utilizing penicillin G (sodium salt), streptomycin sulfate and amphotericin B as Fungizone® antimycotic in 0.085 saline; Invitrogen). Globes were entered through the sclera near the optic nerve with a blade and the lens was gently extruded by cutting the sclera and pulling outward on the cut edges. A fine pair of forceps was used to remove any remaining ciliary body from around the lens equator. The appearance of all lenses and lens capsules was examined under a microscope. Most of the lenses appeared healthy, transparent and undamaged, with the exception of one or two lenses that showed mild signs of cataract formation.

2.3. Lens squeezing methods

Squeezing of the lenses was started about 5–10 min postmortem. The mouse lens squeezing tests were conducted in two ways; 1) using a simple incremental microscope slide cover-slip test or, 2) using a fully automated lens squeezer system.

2.3.1. Cover-slip method

Each lens was individually placed in a transparent glass chamber filled with room temperature HBSS. The lens was positioned in a 400 μm deep, 2200 μm diameter milled indentation in the Plexiglas base of the chamber. A 22 mm square glass microscope slide cover-slip (Corning, Product #2865-22) was placed with one edge resting on the base of the chamber and the opposite edge of the cover-slip just resting on the mouse lens (Fig. 1A). A cut glass slide was placed against the bottom edge of the cover-slips to prevent the cover-slips from sliding off the lens. After each cover-slip was placed on the lens, a high magnification digital image of the lens was captured using a digital charge-coupled device (CCD) camera (The ImagingSource, DMK 21BU04) mounted to the side of the chamber. Three additional cover-slips were then placed on the first cover-slip, one at a time, to add additional weight to the lens, and an image of the lens was captured and saved to a computer after each cover-slip was added. Images were subsequently analyzed for a change in horizontal lens diameter as a function of the cover-slips placed on the lens. The force in grams exerted by the edge of a cover-slip was estimated by resting the edge of a cover-slip on a scale in the same orientation as the cover-slip rested on the mouse lens during the lens testing process. The consistency of the weights of various cover-slips was determined by weighing 10 cover-slips from the same box.

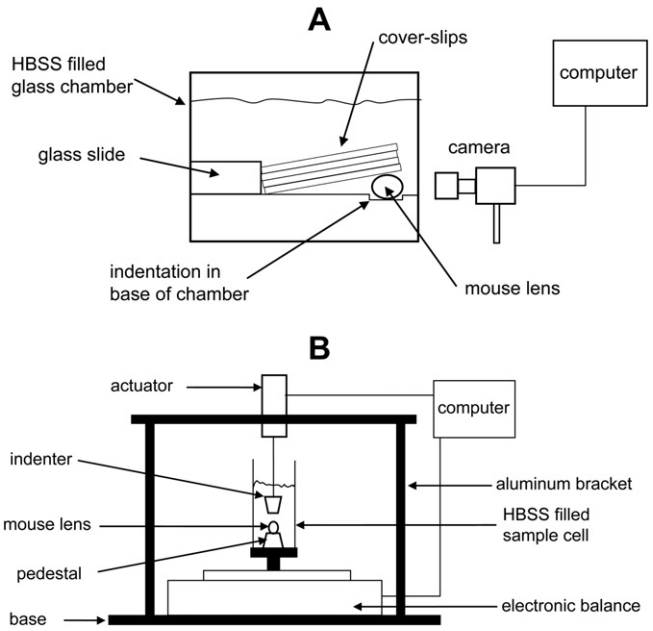

Fig. 1. Schematic drawings of A) the cover-slip test and B) the automated squeezer device. Not drawn to scale.

2.3.2. Automated squeezer method

The mouse lens was placed on the flat, 2 mm diameter upper flat surface of a conical pedestal placed in the bottom of a rectangular and flat sided, 25 ml sample cell (Hach Product # 2410212) filled with room temperature HBSS (Fig. 1B). All lenses were positioned with the optical axis vertically oriented. This was observed under a microscope as lenses were positioned and also in the live view of the lens through the video camera.

An actuator (LTA-HS Precision Motorized Actuator, Newport) with a range of 0–50 mm was mounted above the mouse lens in a solid aluminum bracket. A conical indenter with a flat tip 2 mm in diameter facing down was affixed to the end of the actuator. The actuator was moved down until the flat tip contacted the mouse lens to apply compressive forces. The actuator was capable of a maximum speed of 5 mm/s. Both the indenter tip and pedestal were made from VisiJet SR-200 plastic material with an InVision™ SR 3-D printer. The sample cell with pedestal and mouse lens was placed on a calibrated electronic laboratory balance (CPS323s, Sartorius) that was used to measure force responses during a squeeze experiment. The output from the balance was fed to the computer via the RS-232 port. The balance had a resolution of 1 mg and a maximum range of 320 g. A CCD camera (Cohu, Model 4912) fitted with a 50 mm TV lens (f 1:1.8, Cosmicar) and a 40 mm TV lens extension tube (Cosmicar) was mounted to the side of the sample cell to give a highly magnified view of the mouse lens positioned on the flat apex of the conical pedestal. Software to control the system was written in MATLAB (R2007a, Mathworks). The software controlled the vertical movement of the actuator via a Motion Controller/Driver (SMS-100 series, Newport, Inc) and recorded the output from the laboratory balance at 5 Hz via the RS-232 port and

captured an image via the camera of the lens being squeezed at several predetermined time-points during the entire procedure.

Three different loading and unloading protocols were tested with the automated system.

The first protocol involved driving the actuator at a fixed, relatively slow rate onto the lens and measuring the resultant force applied on the balance through the lens. With this protocol a 10 mg preloading force was first applied to the lens. Preloading established a common start point for all the lenses tested and was performed as an automated part of the procedure prior to the actual testing. Preloading was performed by an automated feedback control algorithm which incrementally moved the actuator down on the lens at a rate of 0.5 μm/s while recording the force exerted on the lens until the desired preloading force was achieved. In this testing protocol, the actuator was first moved down onto the lens at a rate of 5 μm/s to the desired displacement and then moved up off the lens again at the same rate. Five different displacements were sequentially tested (displacements from 50 to 250 μm in 50 μm increments). For each displacement, two cycles were repeated with a 20 s interval. This produced time–force curves for each displacement and from this, force–displacement curves could be plotted (Fig. 2). In this testing protocol, no images were captured during the squeezing process.

The second protocol also required a preload followed by a rapid (5000 μm/s) displacement of the actuator in three discrete steps

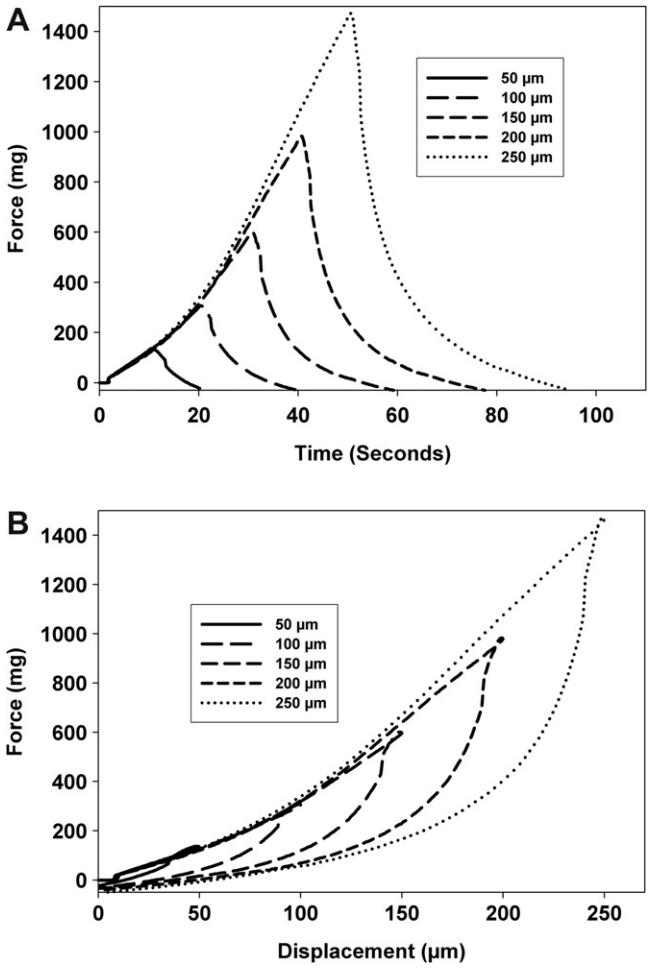

Fig. 2. A) A family of force response curves as a function of time from five different displacements after preloading. B) The same data plotted as force–displacement curves shows the relative consistency of the increasing displacement responses, but the increasing hysteresis in the return path. Data shown is from an approximately 9-month old mouse lens.

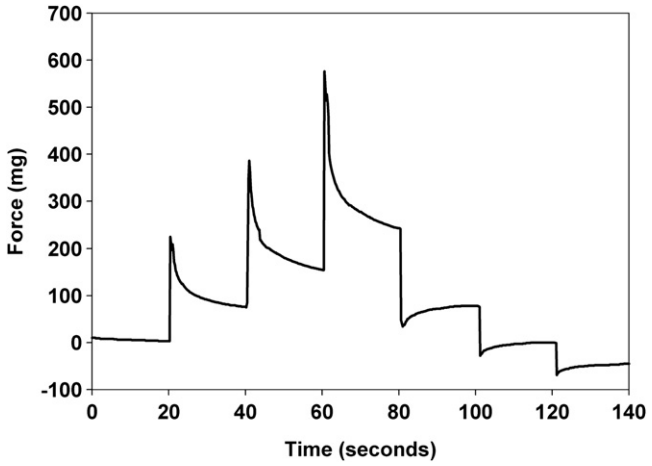

Fig. 3. Force response from a step-wise displacement increment. Data was from an approximately 9-month old mouse lens.

first moving down onto the lens and then moving up off the lens. After each step there was a wait period of 20 s. In this protocol, the magnitude of the step displacements was kept constant. Results were analyzed as force response versus time curves (Fig. 3).

The third protocol consisted of a series of incremental loading steps to achieve pre-determined actuator generated forces on the lens followed by a series of unloading steps. This was accomplished by moving the actuator at a constant rate of 7 μm/s until the desired

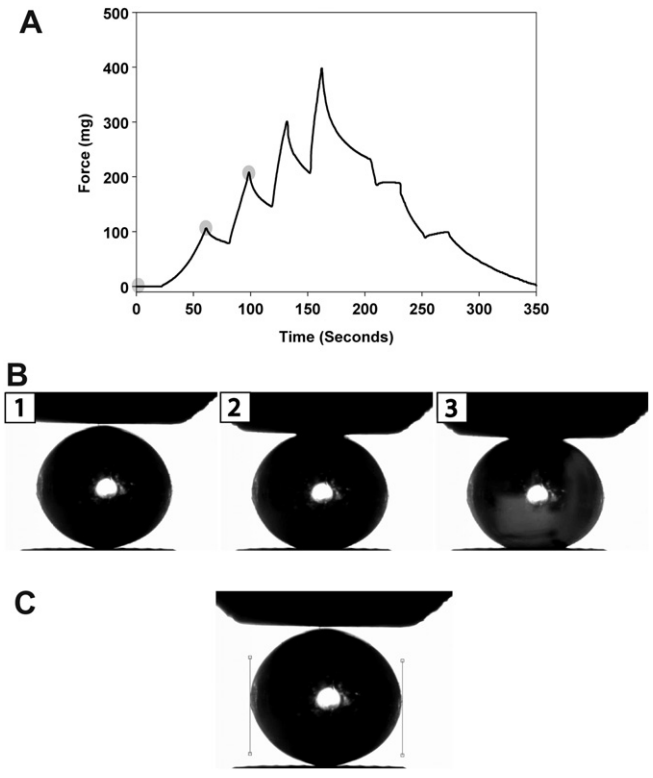

Fig. 4. A) Force response from running the actuator until the desired force was achieved (protocol 3 with the automated squeezer). Circles represent the time points at which the three images shown below were captured. B) Images of mouse lens between the indenter above and the pedestal below, obtained during an automated squeezing experiment; 1) no force, 2) 97 mg force and 3) 194 mg force. C) Image showing how lens diameter was measured using Matlab. The diameter in pixels was obtained by subtracting the *x*-values of the lines on the image. Data and images shown are from a 9-month old mouse lens.

force was achieved. Once this desired force was achieved a 20 s wait period followed to allow for observations of creep of the lenses. During this wait period three images were captured at the 0, 10 and 20 s time points. The analysis presented was for the 0 s time point images, but no systematic difference was observed for images from 0, 10 and 20 s. No preloading was done prior to these tests. Force increments of 97 mg were used to match the force determined from a single cover-slip in the cover-slip method. The forces used were 97, 194, 291 and 388 mg. This was done to permit a direct comparison between the automated squeezer method and the incremental cover-slip method. A complete cycle involved incremental loading to four different force values followed by incremental unloading. One complete run took 15–20 min.

2.4. Data collection

Force and displacement data from the balance and actuator respectively was collected through a RS-232 port and a USB port using a USB to COM port adapter (SMC-USB, Newport) at a frequency of 5 Hz and stored on the computer for later analysis (Fig. 4A). Images were captured with a digital FireWire camera and saved to disk during the experiment immediately after each desired force was attained and additional images at ten and twenty seconds thereafter (Fig. 4B). Images were subsequently analyzed for change in horizontal diameter as a function of the applied squeezing force. Data obtained from the third protocol of the automated squeezer described above was compared to the data from the cover-slip method described above.

2.5. Graphing and statistics

To compare the young and old lenses, the change in horizontal diameter at each force was measured and averages calculated from the total lens population for each group. Differences between the different populations were tested for statistical significance using unpaired (due to unequal numbers) *t*-tests. Force and displacement data was plotted to compare the displacement needed for a given force when loading onto a young lens versus loading onto an old lens.

2.6. Measurements of change in diameter of the lens

Images of the lenses were analyzed to measure lens diameters using MATLAB. For each force applied to the lens the corresponding image was selected and the horizontal diameter measured. The horizontal diameter was measured in pixels by drawing vertical lines on the left and right margins at the lens equator (Fig. 4C) and recording the difference in the *x*-coordinate positions of these two lines. A micrometer ruled grid image was captured at the same magnification and focus at the end of each experiment to convert pixels to micrometers.

2.7. Data and analysis

Although several methods were developed and described above, only data and analysis from the covers-slip method and the third protocol of the automated squeezer method are presented here. The number of 7–9 month old retired breeder lenses tested with the cover-slip method and the third protocol of the automated squeezer was 18 and 10 respectively. The number of 4-week old mice lenses tested using the cover-slip and third protocol of the automated squeezer was 10 and 9 respectively.

2.8. Confocal imaging of mouse lens squeezing

To determine the effect of squeezing the mouse lenses, at a cellular level, imaging was performed while squeezing mouse

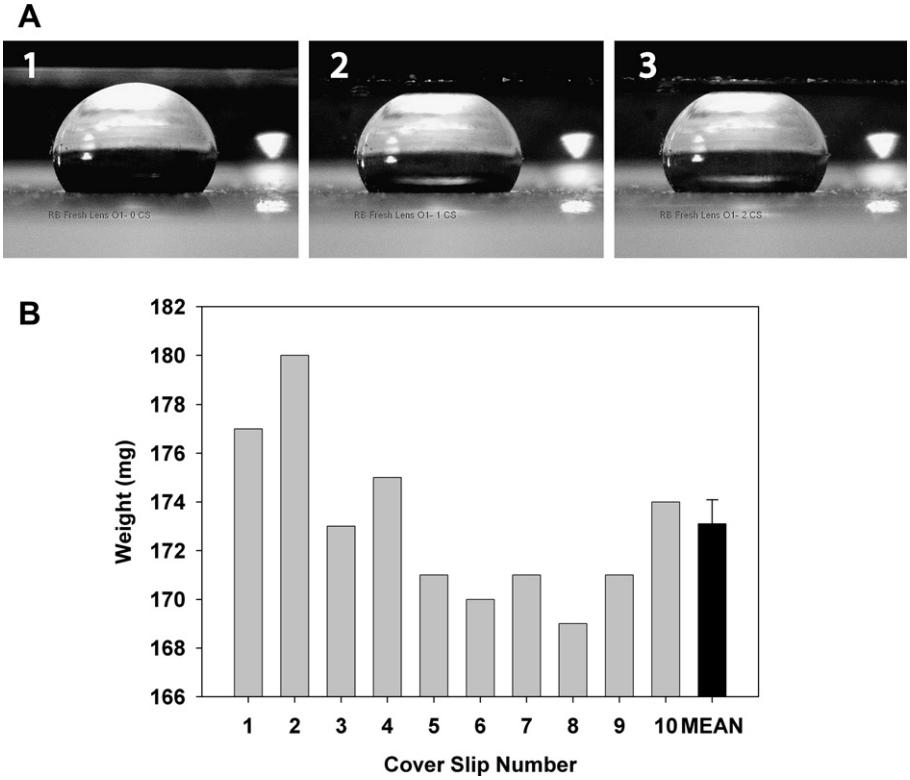

Fig. 5. A) Images from the cover-slip test showing the side view of a mouse lens with 1) no cover-slip, 2) 1 cover-slip, 3) 2 cover-slips. The flattening of the mouse lens and the increase in lens diameter can be seen and was measured from the images. Images are from 9-month old mouse lens. B) Weights of 10 cover slips with their mean and standard error shown.

lenses under a confocal microscope (HRT, Heidelberg Engineering) with the HRT Rostock Cornea Module imaging lens. This is a confocal microscope with a contact applanation lens designed for high resolution corneal imaging. To use the HRT on mouse lenses, the HRT with the Rostock Cornea Module was mounted vertically attached to a micrometer controlled linear stage (Newport Corporation). The Plexiglas base plate with the circular indentation (described above in the cover-slip method) was placed under the HRT. The mouse lens was placed in the indentation with the optical axis vertically oriented. A drop of HBSS was placed over the mouse lens. The HRT was lowered until it just contacted the mouse lens. Sequences of 100 images were captured as the HRT was driven down onto mouse lenses by 100–200 μm.

3. Results

The force that the edge of a cover-slip exerts was determined to be 97 mg with one cover slip. Multiples of this force was considered to be exerted when two, three and four cover-slips were placed on the lens. The addition of successive cover-slips to a mouse lens resulted in successive squeezing, flattening and increase in horizontal diameter of the mouse lenses (Fig. 5A). Subsequently, after weighing 10 different cover-slips from the same box, it was established that the individual cover-slips varied in weight between 169 and 180 mg (Fig. 5B).

Horizontal diameters were smaller for lenses from the younger mice (range: 2.03–2.37 mm; mean 2.23 mm; std ± 0.145) compared to lenses from the older retired breeders (range: 2.45–2.60 mm; mean 2.51 mm; std ± 0.041).

3.1. Comparison between the cover slip method and the automated squeezer

The results from the cover-slip method and third protocol of the automated squeezer system were compared in their assessments of lens stiffness and age-dependent differences. For lenses from 4-week old mice, the change in horizontal lens diameter between the two methods was similar. *P*-values at 97, 194, 291 and 388 mg force values were 0.75, 0.23, 0.069 and 0.14 respectively showing there was no statistically significant difference between the cover-slip method ($n = 10$) and the third protocol of the automated squeezer ($n = 9$) for the 4-week old lenses (Fig. 6A). The greatest difference between the two methods occurred at step three and four for the 4 week old mouse lenses where the differences between the two methods were 21.60 and 23.58 μm respectively. For the older mouse lenses *p*-values at 97, 194, 291 and 388 mg force values were 0.03, 0.30, 0.17, 0.70 respectively. A significant difference between the cover-slip method ($n = 18$) and the third protocol of the automated squeezer method ($n = 10$) was only seen for the 97 mg force with an average change in horizontal diameter between the two methods of 8.3 μm (Fig. 6B).

The standard errors of the means of all the lenses tested with the automated squeezer were generally smaller than those from the cover-slip method (Tables 1 and 2).

3.2. Differences in mechanical properties between young and old mouse lenses

The average change in horizontal diameter for the lenses from 4-week old mice was greater than for the lenses from the older mice at each successive force level. The changes in diameters between young and old lenses were significantly different for all four force values with *p*-values less than 0.001 for both the automated squeezer and cover-slip methods. The average diameter change was about three times greater for the younger mouse lenses than for the older lenses using both the cover-slip test and the automated squeezer (Fig. 7A and B).

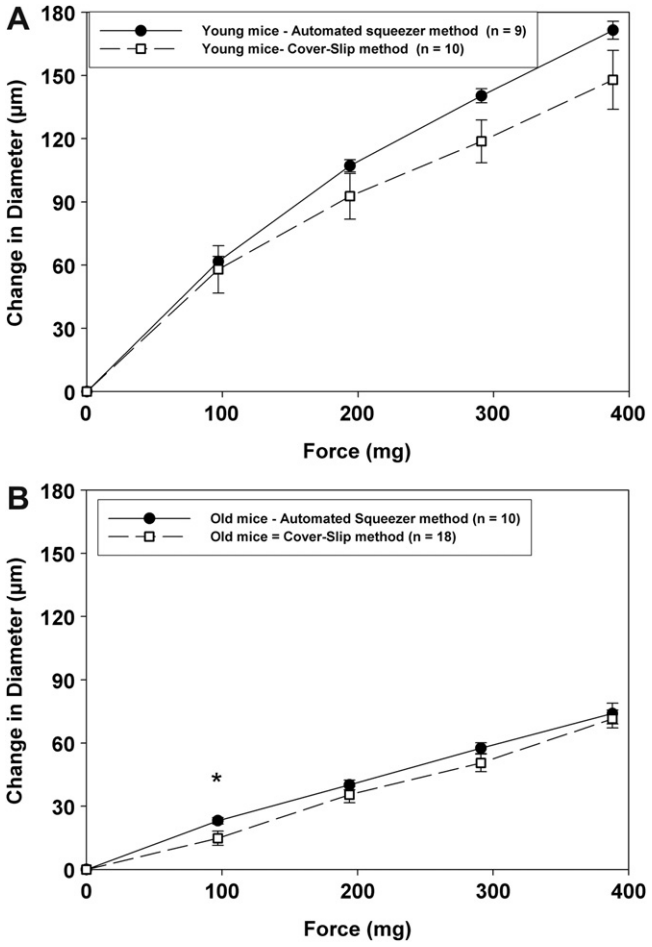

Fig. 6. Comparison of the average change in lens diameter using the automated squeezer and the cover-slip test as a function of force. A) Young mouse lenses; *p*-values were: for 97 mg: 0.75; for 194 mg: 0.23; for 291 mg: 0.069; for 388 mg: 0.14. No significant differences were found at all forces. B) Old mouse lenses; *p*-values were: for 97 mg: 0.03; for 194 mg: 0.30; for 291 mg: 0.17; 388 mg: 0.70. The asterisk denotes a statistically significant difference at 97 mg force only. Error bars are ±1 SEM.

Force–displacement data from the third protocol of the automated squeezer method was also analyzed to show the differences between old and young mouse lenses. To attain a given force, the actuator had to undergo a greater displacement when loading onto a young mouse lens compared to an old mouse lens (Fig. 8A). A *t*-test on the displacement, at all four force values used, indicated significance with *p*-values less than 0.001. In addition, the change in diameter of the lenses for the automated squeezer method was analyzed against the displacement of the actuator (Fig. 8B) to

Table 1
Summary of the horizontal diameter changes obtained in the lenses from the 4-week old mice using the automated squeezer and cover slip methods.

Force (mg)	Corresponding # of cover slips	Avg. change in diameter Automated squeezer method (μm)	Std error	Avg. change in diameter cover slip method (μm)	Std error
97	1	61.75	2.36	57.98	11.20
194	2	107.14	2.86	92.65	10.86
291	3	140.31	3.34	118.71	10.17
388	4	171.46	4.23	147.89	13.96

Table 2
Summary of the horizontal diameter changes obtained in the lenses from the retired breeders using the automated squeezer and cover-slip methods.

Force (mg)	Corresponding # of cover slips	Avg. change in diameter Automated squeezer method (μm)	Std error	Avg. change in diameter Cover slip method (μm)	Std error
97	1	23.10	1.52	14.80	3.43
194	2	40.12	2.27	35.46	3.81
291	3	57.54	2.61	50.54	4.18
388	4	73.97	4.92	71.43	4.23

emphasize the difference in the both the displacement required and the average change in diameter between young male mice and old male mice lenses. Both the displacements and the changes in diameter were statistically significant between the young and old lenses with p-values less than 0.001.

Confocal imaging of the mouse lens during squeezing showed that displacements of 200 μm onto the lens caused the cortical layers of the lens, but not the capsule, to separate at the suture plane (Fig. 9). As the increasing displacement is applied to the lens, the cellular structure holding the lens suture together is broken as the cortical regions of the lens separates at the suture (Movie 1). This separation of the lens is initially restricted to the lens suture region, presumably indicating this is the weakest region of the lens. With increasing displacements, as the suture opens further, the lens cortical layers begin to separate outside the suture region. This does not result in gross anatomical changes in the lens or loss of lens transparency after squeezing, but the amount of squeezing applied cannot be considered non-destructive.

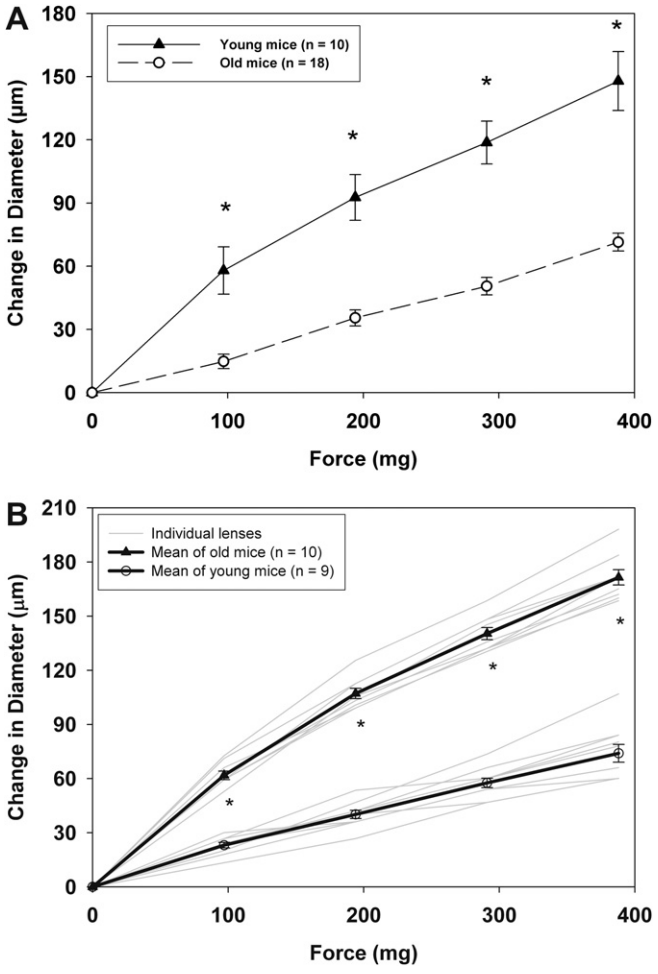

Fig. 7. Computed average change in diameter (micrometers) on application of force for young mouse lenses compared to older mouse lenses using A) the cover-slip method (asterisks denote statistical significance; p-values: for 97 mg: $p < 0.001$; for 194 mg: $p < 0.001$; for 291 mg: $p < 0.001$; for 388 mg: $p < 0.001$) and B) the third protocol of the automated squeezer method with raw data from the individual lenses plotted (asterisks denote statistical significance; p-values: for 97 mg: $p < 0.001$; for 194 mg: $p < 0.001$; for 291 mg: $p < 0.001$; for 388 mg: $p < 0.001$).

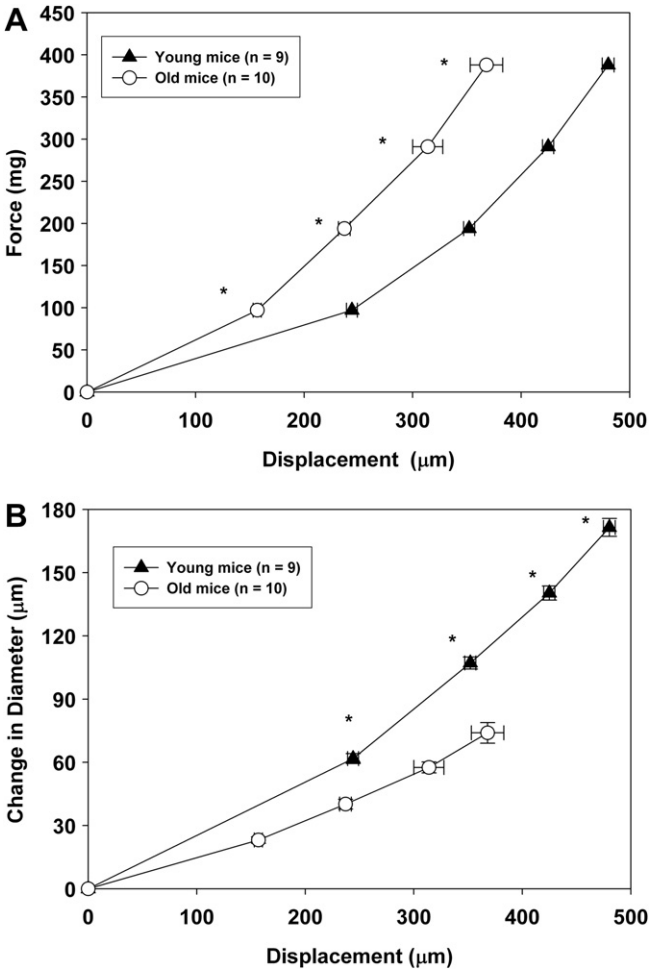

Fig. 8. A) Force as a function of actuator displacement curves from young and old mouse lenses using the third automated squeezer protocol (asterisks denote statistical significance; p-values: for 97 mg: $p < 0.001$; for 194 mg: $p < 0.001$; for 291 mg: $p < 0.001$; for 388 mg: $p < 0.001$). B) Average change in diameter plotted against the average displacement of the actuator for the young and old mouse lenses (asterisks denote statistical significance; p-values: for 97 mg: $p < 0.001$; for 194 mg: $p < 0.001$; for 291 mg: $p < 0.001$; for 388 mg: $p < 0.001$) for both variables.

4. Discussion

The purpose of this study was to use different squeezing techniques to understand their benefits and drawbacks and to compare lens stiffness of 4-week old and 8–9 month old male mice.

It is of interest to understand the nature of the squeezing that is applied on the lenses. The young mouse lenses were between 2030 and 2370 μm in diameter and 500 μm of squeezing is therefore approximately 25% of the lens diameter. The old mouse lenses were between 2450 and 2600 μm in diameter and 500 μm of squeezing is therefore approximately 20% of the lens diameter. It is not clear

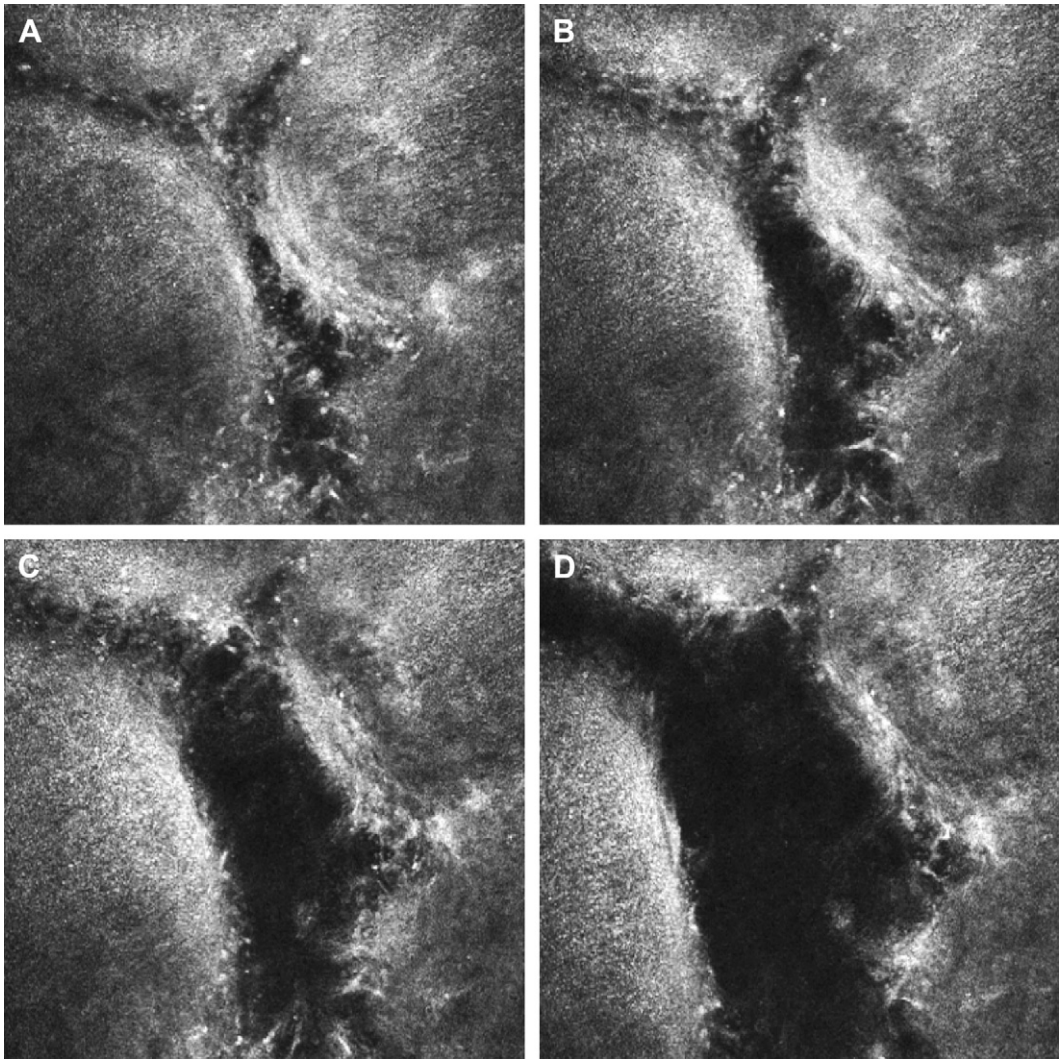

Fig. 9. Confocal images captured during a sequence of 0–200 μm squeezing of a 4 week old mouse lens. The sequence of images A–D shows the progressive separation of the mouse lens suture as the confocal microscope was displaced onto the lens. Image dimensions are 383 μm × 383 μm.

how deep the cortical layers extend and at what depth in the mouse lens the nuclear fibers can be considered to begin. However, if the lenses are being squeezed by approximately a quarter of their diameter, this represents a significant deformation and therefore it can reasonably be concluded that this amount of squeezing impacts both cortical and nuclear regions of the lens. The smaller magnitudes of squeezing also showed significant differences between the young and older lenses. Smaller displacements onto the lens would certainly have been less destructive. The confocal imaging demonstrates that the lens sutures were separating at 200 μm and therefore this still remains somewhat destructive in nature. The amount of squeezing applied here may be particularly destructive for mouse lenses that are relatively stiff and do not undergo accommodative changes in shape as do young primate lenses. Similar magnitudes of mechanical squeezing in younger primate lenses would likely be non-destructive and may be more representative of a physiological range of deformation that the lens might be expected to undergo with accommodation. Squeezing lenses in which the capsule remains intact also necessarily includes mechanical effects due to the capsule. The differences between the younger and older lenses reported here would include differences in mechanical properties of the capsule as well as differences in the lens itself. Studies measuring localized stiffness in human lenses show that the age-related increase in stiffness of the lens occurs in both the cortex and the nucleus, but with a disproportionally greater increase in stiffness in the nucleus (Heys et al., 2004; Weeber et al., 2007). These prior tests on human lenses were also destructive since the human lenses were cut in half and a transducer was forced into the cut surface of the lens which would be composed of cut and damaged lens fiber cells. Non-destructive testing of whole human lenses also showed an age-related exponential increase in stiffness (Glasser and Campbell, 1999), but permits no differentiation between cortex and nucleus. The results from this study on mouse lenses do not provide the opportunity to distinguish relative stiffness between the capsule, cortex and nucleus, but they do show a significant increase in stiffness of the lenses from old mice compared to younger mice.

The first automated squeezer protocol produced a family of force/time curves (Fig. 2) which show a non-linear, but systematically increasing force with a constantly increasing displacement. The force achieved over the full range of displacements for each trial could be used to compare young and old lenses. This third automated squeezer protocol allows for a general comparison of lens stiffness between two groups of lenses using the curves obtained. The time/force curves also provide the opportunity to observe the changes as force/displacement curves and these show

the hysteresis that occurs between the increasing vs. decreasing displacement. A relatively slow actuator movement of 5 μm/s was used for this testing but despite the slow speed, the lens remodeling after squeezing still lagged behind the actuator movement on the return phases as can be observed by the hysteresis reflecting reduced force for a given displacement. This indicates that as the lenses were initially squeezed, the lens undergoes a non-elastic deformation and that it takes some time for the lenses to recover. This too may be an indication that the testing, even for these relatively small displacements, is destructive. Even so, the force–displacement curves travel along very similar paths during the successively increasing squeezing phases, indicating that the results from the repeated squeezing is reproducible.

In the second automated squeezer protocol, the actuator moved relatively rapidly in discrete steps and then remained stationary until the next step. As the actuator moved down onto the lens there was a rapid increase in the force which then decayed exponentially over time until the next actuator step. This exponential decay is likely due to creep as the lenses undergo some remodeling and change in shape under the constant force from the actuator. This progressive creep makes it difficult to identify a single force value for each successive step for comparing young and old lenses.

With the third automated squeezer protocol, all lenses were loaded to the same force steps unlike the previous protocols where the actuator displacement was the same for each successive step, but the force varied. In this protocol, the displacement of the actuator on the lens was designed to mimic placing a cover-slip onto the lens. Lens images were captured at each force step as was done for the cover-slip method after placing each successive cover-slip on the lens. Images were analyzed in the same way for these two different tests. Although similar force steps in multiples of 97 mg were used to allow a comparison between the two methods, subsequent testing demonstrated variability of the weights of individual cover-slips. This may account for some of the greater variance in the cover-slip method compared to the third protocol of automated squeezer method. In addition, once a cover slip is placed on a lens, it continues to exert a force on the lens and with the observed creep, if the image is captured later the lens diameter may have changed more than if the image was captured sooner. This is unlike that with the automated system when the actuator stops moving down onto the lens once the desired force is achieved and then maintains a constant and unchanging position on the lens. Further, in the automated system, the image was captured as soon as the desired force was achieved. This too could provide an explanation for the reduced variance of the automated system compared to the cover-slip method. Measuring the change in lens diameter in the two methods allowed a comparison between the two methods.

The conclusions drawn from the average change in lens diameter were corroborated by the force–displacement data obtained from the third protocol of automated squeezer method. The change in lens diameter and the displacement curves both show a significant difference between the young and old mouse lenses. There was a greater change in diameter and a greater displacement of the actuator when loading on the young mouse lenses compared to the old mouse lenses. Both these trends indicated that the lenses from the older male mice were stiffer compared to the lenses from the younger male mice.

Although the number of lenses tested with these methods was relatively small, both these methods show statistically significantly differences in the change in diameter on application of forces between the young and old mouse lenses. Prior studies in mouse lenses have shown that the number of disulfide bonds increase with increasing age (East et al., 1978). This could be the cause of the increased stiffness in the older lenses. Recent studies suggested that the age-related increase in lens stiffness is due to loss of lens fiber cells soluble alpha-crystallin proteins as the crystallins bind denatured proteins to form high molecular weight aggregates that become insoluble and precipitate out (Heys et al., 2007). The increase in stiffness of the lens closely follows the loss of soluble proteins in the lens with increasing age (Heys et al., 2007).

5. Conclusion

Various methods were evaluated for studying age-related changes in stiffness of mouse lenses. The testing showed that lenses from 9-month old C57BL/6J mice to be stiffer than lenses from 4-week old C57BL/6J mice. The methods used in these tests are reliable and consistent given that results obtained clearly show that the changes in lens diameter were greater for the younger lenses compared to the older lenses. The mouse lens is not a lens that naturally undergoes a change in shape such as with accommodation. Therefore, the extent of squeezing applied to the mouse lenses was likely destructive in nature. However, destructive testing has previously been used to demonstrate the age-related increase in stiffness of human lenses. The methods developed here may not be destructive and may be useful for evaluating age-related changes in stiffness of lenses of species that do undergo accommodative changes in shape as well as being useful for evaluating approaches to soften the lens such as drug or laser treatments.

Acknowledgements

Thanks to Chris Kuether for technical assistance, to Bill Burns and Bill Garner for helpful suggestions on the study methods, to Michael Twa for use of the HRT. This study was funded by a grant from Encore Vision to AG.

Appendix. Supplementary data

Supplementary data associated with this article can be found in the online version, at doi:10.1016/j.exer.2010.06.003.

References

East, E.J., Chang, R.C.C., Yu, N.-T., Kuck Jr., J.F.R., 1978. Raman spectroscopic measurement of total sulfhydryl in intact lens as affected by aging and ultraviolet irradiation. Deuterium exchange as a probe for accessible sulfhydryl in living tissue. J. Biol. Chem. 253, 1436–1441.

Fisher, R.F., 1971. Elastic constants of human lens. J. Physiol. 212, 147–180.

Glasser, A., Campbell, M.C.W., 1998. Presbyopia and the optical changes in the human crystalline lens with age. Vision Res. 38, 209–229.

Glasser, A., Campbell, M.C., 1999. Biometric, optical and physical changes in the isolated human crystalline lens with age in relation to presbyopia. Vision Res. 39, 1991–2015.

Heys, K.R., Cram, S.L., Truscott, R.J.W., 2004. Massive increase in the stiffness of the human lens nucleus with age: the basis for presbyopia? Mol. Vision 10, 956–963.

Heys, K.R., Friedrich, M.G., Truscott, R.J., 2007. Presbyopia and heat: changes associated with ageing of the human lens suggest a functional role for the small heat shock protein, alpha-crystallin, in maintaining lens flexibility. Ageing Cell 6 (6), 807–815.

Hollman, K.W., O'Donnell, M., Erpelding, T.N., 2007. Mapping elasticity in human lenses using bubble-based acoustic radiation force. Exp. Eye Res. 85, 890–893.

Krueger, R.R., Sun, X.K., Stroh, J., Myers, R., 2001. Experimental increase in accommodative potential after neodymium: yttrium-aluminum-garnet laser photodisruption of paired cadaver lenses. Ophthalmology 108, 2122–2129.

Pau, H., Kranz, J., 1991. The increasing sclerosis of the human lens with age and its relevance to accommodation and presbyopia. Graefe's Arch. Clin. Exp. Opthalmol. 229, 294–296.

Sistla, P.A., Reilly, M.A., Andley, U.P., Ravi, N., 2009. The effect of R120G mutation in AlphaB-Crystallin on the mechanical properties of mouse lenses. ARVO Abstract, 2107.

Weeber, H.A., Eckert, G., Soergel, F., Meyer, C.H., Pechhold, W., van der Heijde, R.G.L., 2005. Dynamic mechanical properties of human lenses. Exp. Eye Res. 80, 425–434.

Weeber, H.A., Eckert, G., Gabriele, Eckert, Pechhold, W., van der Heijde, R.G.L., 2007. Stiffness gradient in the crystalline lens. Graefe's Arch. Clin. Exp. Ophthalmol. 245, 1357–1366.